

# Dynamic Analysis of All-Terrain Vehicle Structure

Poula Kamel<sup>1</sup>, George A. Fayek<sup>2</sup>, Ahmed A. A. Saad<sup>3</sup>

1. Assistant Lecturer, Automotive Eng. Department, Faculty of Engineering, Helwan University, Egypt.
2. Researcher, Automotive Eng. Department, Faculty of Engineering, Helwan University, Egypt.
3. Professor of Automotive Eng. Department, Faculty of Engineering, Helwan University, Egypt.

## Abstract

A safety analysis of an all-terrain vehicle space frame used explicit dynamics in this research. The main design objective of such a frame is driver safety while enhancing structure rigidity. Explicit dynamics analysis provides the designer with the effects of the impact on the structure frame members regarding energy, dynamic stress, and acceleration. The tubular frame 3D model is introduced in SolidWorks considering the powertrain system and driver weights. Then, the frame is subjected to a frontal crash scenario to a fixed full-width rigid barrier in the ANSYS workbench. The explicit dynamics model improves the accuracy and computational efficiency of the analysis, however, a validation was used the lumped mass-spring (LMS) system is executed in MATLAB/SIMULINK environment as an alternative computation technique to ensure FEA simulation results. A 3 DOF dynamic model is utilized to investigate the system's equations of motion in the forward direction. Three main zones are considered including the front bulkhead, roll-cage, and rear engine compartment to represent the mass model accelerations. The deflection values of the vehicle frame according to the frontal crash loading condition are studied, however, the frame members' stiffness was measured experimentally. Finally, the two analysis methods were compared for vehicle frame safety evaluation. The results of the explicit dynamics simulation along with the calculated lumped-mass spring system results indicate that the designed space frame achieves the requirements of structure rigidity regarding the frontal crash scenario condition, and the results of the two models satisfy the model rigidity in terms of deflection, energy absorption and vehicle acceleration.

## Keywords

All-Terrain Vehicle Crashworthiness, Explicit Dynamics, ANSYS, Frontal Collision.

## Introduction

The frame design of the all-terrain vehicle must ensure structure rigidity and driver safety. Occasionally, there is little space to design and implement crumple zones in most vehicles, especially in the frontal section since most crashes occur in this area. Therefore, the design of the tubular space frame members must play a vital role in dissipating the crash energy and mitigating the effect of the impact on the driver. The frame dynamic behavior in terms of deformation, deceleration, and absorption energy during crashes is considered a sophisticated problem due to the very short time of action. The predictability of the frame behavior can largely support the efficiency of the product design and implementation. Nevertheless, many approaches have been developed to encounter this problem. crash modeling methodologies can be categorized as reduced-order dynamic models, multi-body models, non-linear finite element models, response surface models, and crash pulse models [1]. Hybrid methods can also be used to approach the same problem. The adoption of the FEA technique to solve stresses generated on the vehicle frame through using CAD software promoted this issue many years ago [2] while Static stress analysis is considered a simple and efficient technique to study such a space frame [2-4].

Explicit dynamics enhance the analysis of mechanical stresses on the frame members in these extreme situations in a way that allows the designer to validate the rigidity of the frame to ensure driver safety. Explicit dynamics is a time integration method used to perform dynamic simulations when speed is important. Explicit dynamics account for quickly changing conditions or discontinuous events, such as free falls, high-speed impacts, and applied loads [6], [7]. However, explicit dynamics simulation requires a large amount of CPU time. So, in many cases, the use of implicit dynamics is preferred when CPU processing hardware is low. Utilization of explicit dynamics simulation in crash models was investigated in many research studies as in [8-11]. However, LMS models as a reduced order dynamic technique can provide a mathematical approach to determine the behavior of vehicle masses with a compromise between hardware quality and results accuracy. For lumped mass-spring (LMS) models, the conventional method is to represent bodies as concentrated point masses coupled by linear or non-linear springs. The force-deformation and force-velocity curves that characterize springs indicate how a force is applied to cause them to deform [12], [13]. Since its initial introduction in the early 1900s for automobile suspension design, this method has been widely applied in the development of automobiles. In such kind of modeling many assumptions are adopted regarding the direction of masses displacements, and distribution of vehicle weight [14]. These assumptions cause a lack of accuracy in the generated model results. The data regarding frame members' stiffness behavior during the exertion of the crash forces cannot be easily determined. So, experimental testing for the frame members could be used as a measuring technique to determine their practical characteristics. Then, the stiffness values of the frame members could be calculated based on the relation between the exerting force on the member and the deflection that occurred.

In this study, a 3D model for the all-terrain vehicle frame is constructed in SolidWorks and simulated using explicit dynamics via FEA ANSYS software during the scenario of the frontal crash at 40 km/h. Construction of an LMS model is obtained to validate the vehicle's dynamic behavior with an alternative strategy. However, a practical approach has been used as a technique for inducing the relation between the exerting force on the members and the resulting deflection. Then, the stiffness values for each member type of the tubular frame were calculated. The results of the models (FEA and LMS) and the experimental work are illustrated in detail in the results section.

### Finite Element Modeling

A finite element model is developed using ANSYS explicit dynamics to numerically simulate the behavior of the all-terrain vehicle structure during a frontal collision. The structure is modeled using first-order shell elements; quad4 and tri3 elements. Thin-walled frame members are efficiently represented using shell finite elements rather than 1D beam or truss elements. 2D finite elements offer numerous benefits over beam elements. Table 1 shows model statistics. Limited options are available for selection due to the local market availability. The cross-sections used for primary and secondary frame members have been selected as obtained in Table 2.

**Table 1 Ansys model statistics**

Number of elements	21994
Number of nodes	21469
Element Size	14.1 mm
Average Element Quality	89.296%
Element Quality Standard Deviation	0.13422
Average Aspect Ratio (Explicit)	1.2753
Aspect Ratio Standard Deviation	0.34737

**Table 2 The primary & secondary member cross-section.**

Parameter	Outer Diameter (mm)	Thickness(mm)
Primary	42.164	1.651
Secondary	26.67	2.67

During the simulation, the driver's weight is represented as a point mass in the FE model applied to the driver's center of gravity. A mass of 70 kg is remotely attached to four faces where the seat belt fixations are welded to the frame members as shown in Figure 1. Similarly, the drivetrain mass is attached to their brackets fixation faces in the frame members as shown in Figure 2. Additionally, a fixed rigid wall is placed in front of the vehicle frame. A vehicle simulation was performed using a 40 km/hr. velocity initial condition. Collision end time is set to be 0.025 seconds divided into 54-time steps.

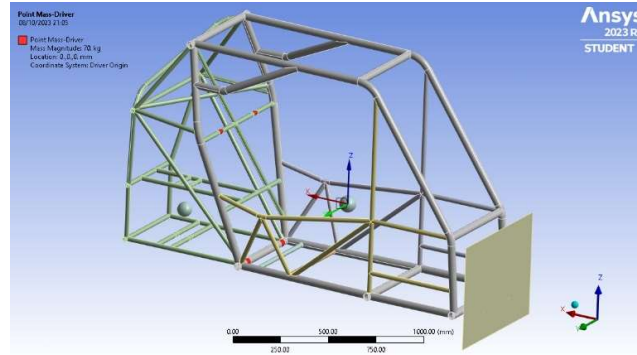


**Figure 1 Seat belt fixation points.**

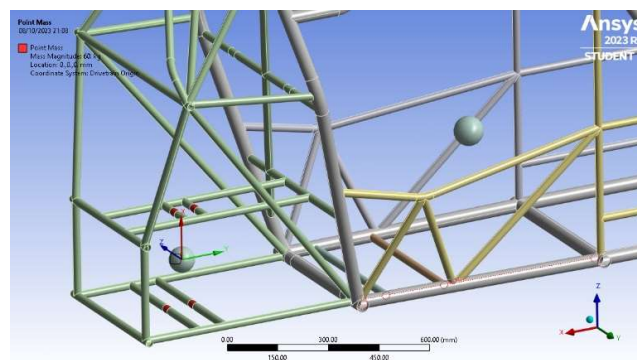


**Figure 2 Drive train fixation points.**

## **Result and Discussions**

### **Finite Element Model Results**

Numerical crash evaluation of a vehicle's structural response employs the finite element (FE) method implemented in ANSYS software. The analysis encompasses a range of impact velocity (40 km/h), assuming an initial undeformed state. Also, A rigid moving barrier is assumed to be hitting the vehicle structure to disregard deformations and stresses within the barrier and to focus on the structure. Additionally, the structure is fully constrained (fixed in all displacements and rotations) at its furthest rear extremities as shown in Figure 3. This approach facilitates isolated investigation of the vehicle's structural behavior under controlled impact scenarios. By employing established numerical techniques and rigorous boundary conditions, valuable insights are observed into the vehicle's crashworthiness and deformation patterns.

The simulation results provided a maximum deceleration of 792.59 m/s<sup>2</sup> in the X-direction and the structure front intrusion is observed to be 102.58 mm at 21.759 milliseconds as shown in Figure 4. Finally, the remaining duration is considered to be vehicle structure rebounding.

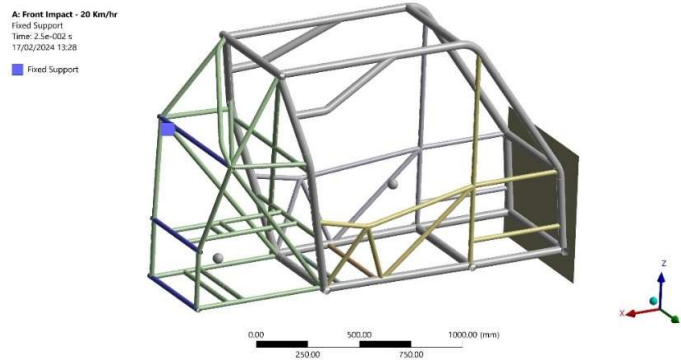
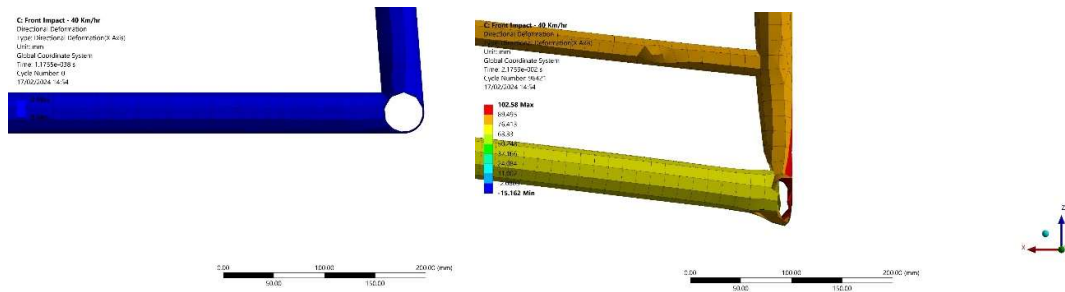


**Figure 3 Fixed supports.**



**(a) Initial zero deformation**

**(b) Deformation at the end**

**Figure 4 Deformation at 40 km/hr.**

## Energy Absorption Results

Investigations are being conducted to determine the maximum energy absorption available in the frontal components of a vehicle during a collision using numerical simulation. However, the stiffness of the front-end members should strike a balance between deformation limits and tolerable deceleration. The balance between the extent of intrusion and the level of deceleration, considering alterations in the structural properties of the vehicle cabin, generates the desired response based on the rigidity and damping following the energy equilibrium described by the Lagrangian equation.

$$T. E. = K. E. - A. E.$$

Where T.E. represents the total energy, K.E. represents the kinetic energy, and A.E. represents the absorbed energy.

The kinetic energy that the vehicle has at a speed of 40 km/h including the structure mass and the driver and drivetrain point masses can be determined as:

$$K. E. = \frac{1}{2}mv^2 = \frac{1}{2}(60.458 + 70 + 60) * 11.1^2 = 11.76 \text{ kJ}$$

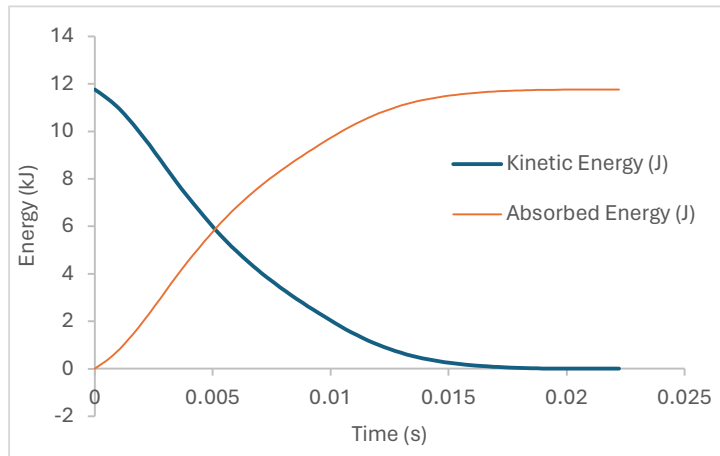


**Figure 5 Energy absorption at impact velocity 40 km/h.**

In a vehicle crash, the speed of 40 km/h decreases because of the resistive elements in the frontal structure. The kinetic energy, which is initially 11.76 kJ, decreases gradually in correlation with the velocity reduction. When the speed reaches zero at 20.4 milliseconds as shown in Figure 5 Energy absorption at impact velocity 40 km/h., the compression phase halts. At this point, all kinetic energy is converted to potential energy in the deformation of the structure components.

### Validation

To validate the ANSYS results, the lumped mass model and experimental data are utilized. The lumped mass model depicts the vehicle frame in a simplified manner, with masses and springs connecting them. The stiffness of these connecting springs is determined through empirical methods. Subsequently, both analytical calculations and empirical data are compared with the ANSYS results for deformation, velocity, and deceleration to validate the simulation findings.

### Experimental Test

A computer-controlled universal testing machine is utilized to conduct compression tests on the structural components of a vehicle, with specifications outlined in Table 3. The collapsed samples are compressed by 100mm at a nominal crosshead speed of 50mm/min, allowing the compression specimens to undergo deformation relative to the applied force, as depicted in Figure 6. The measured outcome is the axial load-deformation relationship, employing the stroke mode operation concept. As shown in Figure 7 four longitudinal specimens are subjected to compression by the crosshead of the universal testing machine to determine the necessary force and achieve the corresponding deformation within a range of 30-100mm of the sample length. In contrast, when a moving vehicle collides with a rigid barrier, the force

required to decelerate the vehicle adheres to the conservation of momentum principle based on the vehicle's mass and velocity in a fully dynamic scenario, occurring over a brief period. This contrasts with the quasi-static test conducted on the Universal Testing Machine, which takes a longer duration to cause the collapse of the structural members' samples.

**Table 3 Universal testing machine specifications.**

		Unit
Manufacturer	JINAN	-
Model	WDW-300	-
Maximum load	300	kN
Test speed range	0.1–250	mm/min
Compression space	700	mm



**Figure 6 Universal testing machine and the resulting output data.**

## Experimental Result and Discussions

Four specimens undergo experimental tests per the proposed methodology, with their characteristics detailed in Table 4. All specimens are constructed from Carbon Steel ASTM A-106 Grade. B., with the characteristics outlined in Table 5. A comparison of the deformation behaviours observed in the experimental tests of the four specimens is illustrated in Figure 8 & Figure 9. It is evident that specimens P1 and S1 demonstrate an axial mode of collapse behaviour, whereas specimens P2 and S2 display a bending mode of collapse.

This study primarily examines the deformation characteristics of thin-walled steel tubes with varying widths under significant axial impact forces. The collapse behavior of the tested samples is influenced by the thickness of the steel tubes as well as the material properties.



**Figure 7 Round HSS samples before the test.**

**Table 4 Mass, geometry, and dimensions of the tested samples.**

Samples	Samples Dimensions (mm)	Mass (kg)
Sample (P1)	HSS 42.164 Dia. x1.3 THK. LG.=300	0.39
Sample (P2)	HSS 42.164 Dia. x1.651 THK. LG.=300	0.49
Sample (S1)	HSS 26.67 Dia. x0.7 THK. LG.=300	0.13
Sample (S2)	HSS 26.67 Dia. x2.67 THK. LG.=300	0.47

**Table 5 ASTM A-106 Grade. B Material properties.**

Parameter	Value	Unit
Density	7850	kg/m <sup>3</sup>
Young's modulus	200	GPa
Poisson ratio	0.3	-
Shear modulus	76.9	GPa
Tensile yield strength	326	MPa
Tensile ultimate strength	517	MPa



**Figure 8 Axial collapse deformation behavior of two samples (P1 & S1).**





**Figure 9 Bending deformation behavior of two samples (P2 & S2)**

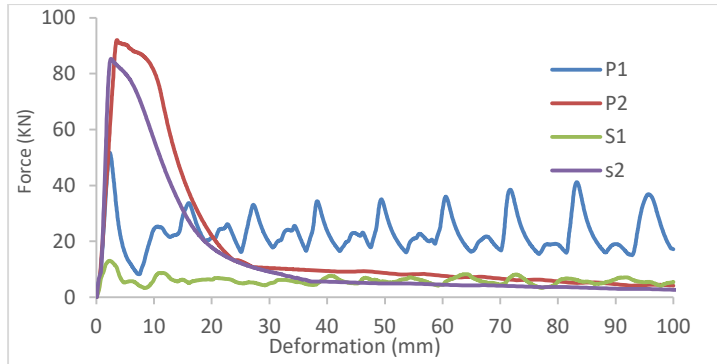


**Figure 10 Force-deformation curves for steel tubes with various design characteristics.**

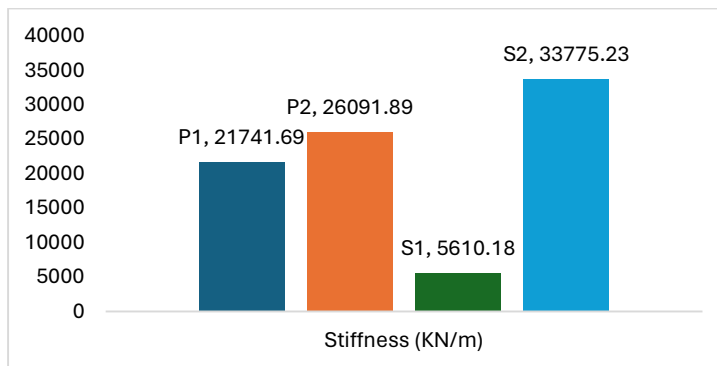


**Figure 11 Results of stiffness coefficients for four samples of carbon steel.**

**P1 & S1 Samples**

The (P1) sample (42.164mm Dia. x 1.3mm THK. LG.=300mm) exhibited a higher energy absorption value, as illustrated in Figure 12. Despite not reaching a high peak force, the consistent mean crush force at moderate levels, as indicated by the observed

collapse behavior, contributed to an increase in energy absorption. A similar pattern is observed with the S1 sample (26.67 Dia. x 0.7 THK. LG.=300mm) but with differing values. In Figure 10 and Figure 11 it is evident that Sample S1 recorded the lowest peak force value (13.01 KN) and stiffness coefficient (5610.18 KN/m).

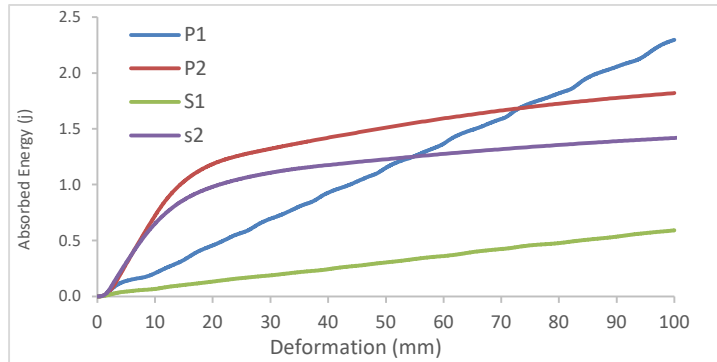


**Figure 12 Energy absorption curves for four samples of carbon steel.**

## P2 & S2 Samples

As shown in Figure 10, Sample P2 with the dimensions of (42.164mm Dia. x1.651mm THK. LG.=300mm) registered the highest value of peak force (92 KN) but the bending behavior of the sample led to minimizing the energy absorption, which reached 1.87 kJ in 100mm of the sample length. On the other hand, sample S2 with the dimensions of (26.67 Dia. x2.67 THK. LG.=300mm) registered the highest value of stiffness coefficient, which is 33775.23 KN/m, and energy absorption 1.2 kJ in 100mm of the sample length.

## LMS Model

The study of the all-terrain vehicle structure in a frontal collision using the mass-spring model concept to estimate the deceleration and intrusion ranges, the model is approximated by a one-dimensional model system. The vehicle structure is represented by three masses that integrate three main zones, front members including pedal box area, roll cage including driver weight and cabin members, and rear engine compartment including drivetrain system. The lumped mass-spring model is considered simple to indicate the collision behavior results. Also, experimental work was performed to determine the characteristics of the structure members' stiffness. The model illustrated in Figure 13 is a 3 DOF System consisting of three lumped masses and 8 nonlinear resistance force elements connecting them. The nonlinear force elements are represented by a piecewise linear function based on different shape functions. For each mass, only one degree of freedom, the displacement in the longitudinal direction is considered, and the state variables are considered by X1, X2, and X3. The LMS model equations are expressed in the equations (1- 6).

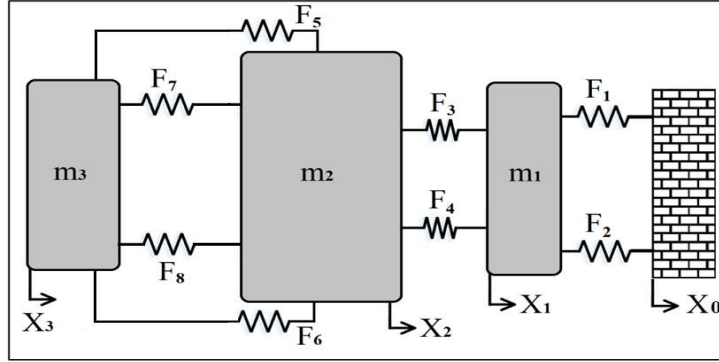


**Figure 13 The lumped mass-spring model of the All-terrain vehicle.**

$$m_1 \ddot{x}_1 - F_{k1} - F_{k2} + F_{k3} + F_{k4} = 0 \quad (1)$$

$$m_2 \ddot{x}_2 - F_{k3} - F_{k4} + F_{k5} + F_{k6} + F_{k7} + F_{k8} = 0 \quad (2)$$

$$m_3 \ddot{x}_3 - F_{k7} - F_{k8} - F_{k5} - F_{k6} = 0 \quad (3)$$

$$m_1 \ddot{x}_1 - [k_1(x_1 - x_0)] - [c_1(\dot{x}_1 - \dot{x}_0)] - [k_2(x_1 - x_0)] - [c_2(\dot{x}_1 - \dot{x}_0)] + [k_3(x_2 - x_1)] + [c_3(\dot{x}_2 - \dot{x}_1)] + [k_4(x_2 - x_1)] + [c_4(\dot{x}_2 - \dot{x}_1)] = 0 \quad (4)$$

$$m_2 \ddot{x}_2 - [k_3(x_2 - x_1)] - [c_3(\dot{x}_2 - \dot{x}_1)] - [k_4(x_2 - x_1)] - [c_4(\dot{x}_2 - \dot{x}_1)] + [k_5(x_3 - x_2)] + [c_5(\dot{x}_3 - \dot{x}_2)] + [k_6(x_3 - x_2)] + [c_6(\dot{x}_3 - \dot{x}_2)] + [k_7(x_3 - x_2)] + [c_7(\dot{x}_3 - \dot{x}_2)] + [k_8(x_3 - x_2)] + [c_8(\dot{x}_3 - \dot{x}_2)] = 0 \quad (5)$$

$$m_3 \ddot{x}_3 - [k_7(x_3 - x_2)] - [c_7(\dot{x}_3 - \dot{x}_2)] - [k_8(x_3 - x_2)] - [c_8(\dot{x}_3 - \dot{x}_2)] - [k_5(x_3 - x_2)] - [c_5(\dot{x}_3 - \dot{x}_2)] - [k_6(x_3 - x_2)] - [c_6(\dot{x}_3 - \dot{x}_2)] = 0 \quad (6)$$

### Comparison Between Finite Element and Lumped Mass Models Results.

Furthermore, ANSYS-generated results were compared with those derived from the LMS model in Figure 14, Figure 15 and Figure 16. The simulation time interval of the models is divided into three stages based on the observed behavior of the structure, and each stage will be discussed in detail as follows.

During the initial stage, which spans from 0 to 0.003 seconds, the collision is initiated. According to Figure 14 and Figure 16, the structure experiences high deceleration rates, reaching its maximum value within 3 milliseconds. Further examination reveals that this time range constitutes 12% of the overall time duration, during which the front member undergoes relatively minor deformation. This phenomenon can be attributed to strain hardening, where the material becomes more

resistant to deformation and stronger as it experiences high strain rates. In the second stage, spanning from 0.003 to 0.015 seconds, the material undergoes yielding, and deceleration stabilizes. This period exhibits a low rate of change of deceleration and increasing values towards zero.

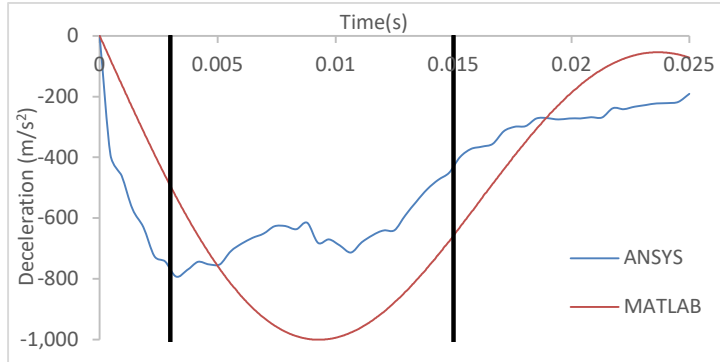


**Figure 14 ANSYS & MATLAB acceleration validation.**

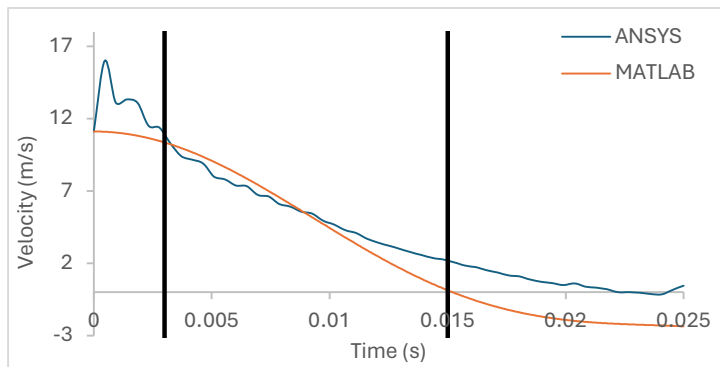


**Figure 15 ANSYS & MATLAB velocity validation.**

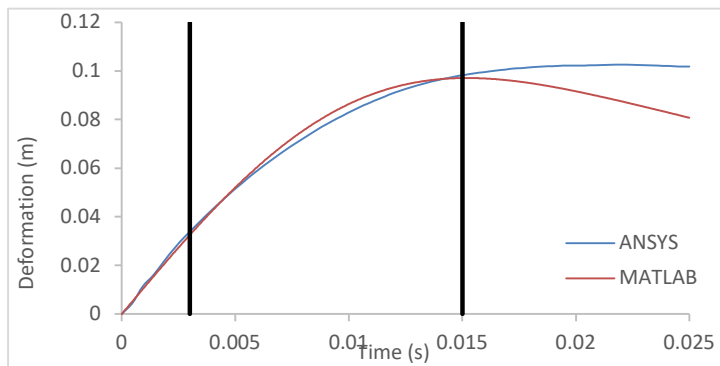


**Figure 16 ANSYS & MATLAB deformation validation**

Consequently, despite experiencing maximum deceleration initially at this stage, the jerk, representing the rate of change of deceleration, is minimal. Additionally, the

velocity decreases during this phase, ensuring reduced risk to driver health and safety over an extended collision duration of this stage.

In the third stage, the vehicle structure's velocity approaches zero, signifying the termination of the collision. With no additional deformation and minimal deceleration values trending towards zero, the collision event concludes, and the vehicle structure rebounds as a whole in the opposite direction due to negative velocity values as shown in Figure 15..

## Conclusions

This work studies the utilization of an explicit dynamics model with the aid of Ansys software to ensure the structure rigidity of a tubular space frame for an all-terrain vehicle structure. First, a CAD model for the vehicle structure is constructed to obtain the main sections of the vehicle including main and secondary tubular members. Secondly, the CAD model is simulated within a front collision scenario using FEA explicit dynamics at speeds of 30 and 40 km/h to ensure its rigidity during the crash. However, to validate the generated model behavior with a substitutional approach to solve the problem, An LMS dynamic model was also built. The structure was abstracted so that only 3-point masses represent the longitudinal motion of the structure during the crash. The LMS model is simulated to test the vehicle for a frontal collision with a rigid barrier at a speed of 40 km/h using the MATLAB/SIMULINK model. The stiffness of the frame members that have been used in the LMS model was calculated based on the experimental work of the members. During this work, main and secondary members were tested using the Universal Testing Machine to induce the relation between the normal force and generated member deflection. The results of the FEA model of the structure simulation are compared to the simulation results of the LMS model. The results of the two models satisfy the model rigidity in terms of deflection, energy absorption and vehicle acceleration.

## References

- [1] G. Noorsumar, S. Rogovchenko, K. G. Robbersmyr, and D. Vysochinskiy, "Mathematical models for assessment of vehicle crashworthiness: a review," *International Journal of Crashworthiness*, vol. 27, no. 5. Taylor and Francis Ltd., pp. 1545–1559, 2022. doi: 10.1080/13588265.2021.1929760.
- [2] N. Noorbhasha, "Computational analysis for improved design of an SAE BAJA Computational analysis for improved design of an SAE BAJA frame structure frame structure," 2010, doi: 10.34917/2016694.
- [3] Y. Chandra, "Design, Analysis and Optimization of a BAJA-SAE Frame," *International Journal of Science and Research*, 2018, doi: 10.21275/SR20208233756.
- [4] P. M. Kamel et al., "Design and Validation of a Light Vehicle Tubular Space Frame Chassis", [Online]. Available: [www.irjet.net](http://www.irjet.net)

- [5] S. Hassaan Abdullah, "Computational Analysis for Optimisation of Baja SAE Roll Cage," 2018. [Online]. Available: [www.ijsrd.com](http://www.ijsrd.com)
- [6] "What is Explicit Dynamics at Ansys?" Accessed: Mar. 22, 2024. [Online]. Available: <https://www.ansys.com/blog/what-is-explicit-dynamics>
- [7] J. M. Chang et al., "Implicit and Explicit Finite Element Methods for Crash Safety Analysis," 2007. [Online]. Available: <https://www.jstor.org/stable/44687867>
- [8] S. Elhussieny, W. Oraby, M. Elkady, A. Abdelhamid, and S. El-Demerdash, "Optimisation of crash dynamics for bus cabin structure based on attained intrusion and deceleration during a frontal collision," *International Journal of Crashworthiness*, vol. 26, no. 5, pp. 501–514, 2021, doi: 10.1080/13588265.2020.1754648.
- [9] "Explicit Dynamic Analysis of Vehicle Roll-Over Crashworthiness Using LS-DYNA," 2006.
- [10] S. Yadav and S. K. Pradhan, "Investigations into dynamic response of automobile components during crash simulation," in *Procedia Engineering*, Elsevier Ltd, 2014, pp. 1254–1264. doi: 10.1016/j.proeng.2014.12.404.
- [11] J. Fehr, P. Holzwarth, and P. Eberhard, "Interface and model reduction for efficient explicit simulations - a case study with nonlinear vehicle crash models," *Math Comput Model Dyn Syst*, vol. 22, no. 4, pp. 380–396, Jul. 2016, doi: 10.1080/13873954.2016.1198385.
- [12] M. M. Kamal, "Analysis and Simulation of Vehicle to Barrier Impact," 1970. [Online]. Available: <https://www.jstor.org/stable/44716186>
- [13] S. M. Ofochebe, C. G. Ozoegwu, and S. O. Enibe, "Performance evaluation of vehicle front structure in crash energy management using lumped mass spring system," *Adv Model Simul Eng Sci*, vol. 2, no. 1, Dec. 2015, doi: 10.1186/s40323-015-0020-1.
- [14] W. Pawlus, H. R. Karimi, and K. G. Robbersmyr, "Development of lumped-parameter mathematical models for a vehicle localized impact," *Journal of Mechanical Science and Technology*, vol. 25, no. 7, pp. 1737–1747, Jul. 2011, doi: 10.1007/s12206-011-0505-x.

## Nomenclature

- a - vehicle acceleration.  
A. E. – Absorbed energy.  
g - gravitational acceleration.  
m - Total mass.  
K. E. – Kinetic energy.  
T. E. – Total energy.  
 $m_1$  - front bulkhead mass.  
 $m_2$  - roll cage mass.

$m_3$ - rear engine compartment mass.  
 $F_1$ - Force generated at the 1<sup>st</sup> member.  
 $F_2$ - Force generated at the 2<sup>nd</sup> member.  
 $F_3$ - Force generated at the 3<sup>rd</sup> member.  
 $F_4$ - Force generated at the 4<sup>th</sup> member.  
 $F_5$ - Force generated at the 5<sup>th</sup> member.  
 $F_6$ - Force generated at the 6<sup>th</sup> member.  
 $F_7$ - Force generated at the 7<sup>th</sup> member.  
 $F_8$ - Force generated at the 8<sup>th</sup> member.  
 $k_1$ - Stiffness of the 1<sup>st</sup> member.  
 $k_2$ - Stiffness of the 2<sup>nd</sup> member.  
 $k_3$ - Stiffness of the 3<sup>rd</sup> member.  
 $k_4$ - Stiffness of the 4<sup>th</sup> member.  
 $k_5$ - Stiffness of the 5<sup>th</sup> member.  
 $k_6$ - Stiffness of the 6<sup>th</sup> member.  
 $k_7$ - Stiffness of the 7<sup>th</sup> member.  
 $k_8$ - Stiffness of the 8<sup>th</sup> member.  
 $c_1$ - Damping of the 1<sup>st</sup> member.  
 $c_2$ - Damping of the 2<sup>nd</sup> member.  
 $c_3$ - Damping of the 3<sup>rd</sup> member.  
 $c_4$ - Damping of the 4<sup>th</sup> member.  
 $c_5$ - Damping of the 5<sup>th</sup> member.  
 $c_6$ - Damping of the 6<sup>th</sup> member.  
 $c_7$ - Damping of the 7<sup>th</sup> member.  
 $c_8$ - Damping of the 8<sup>th</sup> member.  
 $x_0$ - Displacement of the rigid wall.  
 $x_1$ - Displacement of the 1<sup>st</sup> mass.  
 $x_2$ - Displacement of the 2<sup>nd</sup> mass.  
 $x_3$ - Displacement of the 3<sup>rd</sup> mass.  
 $\dot{x}_1$ - Velocity of the 1<sup>st</sup> mass.  
 $\dot{x}_2$ - Velocity of the 2<sup>nd</sup> mass.  
 $\dot{x}_3$ - Velocity of the 3<sup>rd</sup> mass.  
 $\ddot{x}_1$ - Acceleration of the 1<sup>st</sup> mass.  
 $\ddot{x}_2$ - Acceleration of the 2<sup>nd</sup> mass.  
 $\ddot{x}_3$ - Acceleration of the 3<sup>rd</sup> mass.

### **Contact Information**

Poula Magdy Kamel  
Teaching Assistant, Faculty of Engineering, Mataria, Helwan University  
Poula.m.kamel@m-eng.helwan.edu.eg